

Effect of non-specific species competition from total RNA on the static mode hybridization response of nanomechanical assays of oligonucleotides

This content has been downloaded from IOPscience. Please scroll down to see the full text.

2014 Nanotechnology 25 225501

(<http://iopscience.iop.org/0957-4484/25/22/225501>)

View [the table of contents for this issue](#), or go to the [journal homepage](#) for more

Download details:

IP Address: 134.226.254.162

This content was downloaded on 09/05/2014 at 07:49

Please note that [terms and conditions apply](#).

Effect of non-specific species competition from total RNA on the static mode hybridization response of nanomechanical assays of oligonucleotides

Rohit Mishra and Martin Hegner

Centre for Research on Adaptive Nanostructures and Nanodevices, School of Physics, Trinity College, Dublin 2, Ireland

E-mail: martin.hegner@tcd.ie

Received 27 January 2014, revised 23 March 2014

Accepted for publication 3 April 2014

Published 8 May 2014

Abstract

We investigate here the nanomechanical response of microcantilever sensors in real-time for detecting a range of ultra-low concentrations of oligonucleotides in a complex background of total cellular RNA extracts from cell lines without labeling or amplification. Cantilever sensor arrays were functionalized with probe single stranded DNA (ssDNA) and reference ssDNA to obtain a differential signal. They were then exposed to complementary target ssDNA strands that were spiked in a fragmented total cellular RNA background in biologically relevant concentrations so as to provide clinically significant analysis. We present a model for prediction of the sensor behavior in competitive backgrounds with parameters that are indicators of the change in nanomechanical response with variation in the target and background concentration. For nanomechanical assays to compete with current technologies it is essential to comprehend such responses with eventual impact on areas like understanding non-coding RNA pharmacokinetics, nucleic acid biomarker assays and miRNA quantification for disease monitoring and diagnosis to mention a few. Additionally, we also achieved a femtomolar sensitivity limit for online oligonucleotide detection in a non-competitive environment with these sensors.

Keywords: microcantilevers, oligonucleotide detection, non-specific competition, total RNA

(Some figures may appear in colour only in the online journal)

Introduction

The detection and quantification of short, single stranded DNA (ssDNA) or RNA molecules (oligonucleotides) with high specificity is of primal importance in functional genomics right from gene expression profiling to the nascent field of small non-coding RNA (ncRNA, 19–24 nucleotides in length) discovery and profiling [1]. This category of RNAs includes small interfering RNA (miRNA and siRNA), transfer RNA, ribosomal RNA and small nuclear and small nucleolar RNA. Functional genomic technologies are directly applied in detection of biomarker transcripts, monitoring of gene expression, elucidating gene function and eventually drug

discovery and patient monitoring. Several technologies [2] that employ arrays of oligonucleotide probes are currently available in this area with DNA microarrays [3, 4] and surface plasmon resonance arrays [5] leading the way. Microcantilever based nanomechanical sensors are a rising class of sensor arrays for bioassays and have made rapid progress in recent years for application towards detection of biological entities [6–11]. They have provided a label-free real time technology with high specificity that has enabled the detection of proteins [12], oligonucleotides [13], viruses [14], bacterial species [15] and fungi [16] among others. They are generally operated in two different modes i.e. static and dynamic mode. The static mode of detection based on surface events that

induce stress changes leading to cantilever deformation has been developed for detection of oligonucleotide sequences with high selectivity and single nucleotide polymorphisms (SNP) sensitivity [13–17]. This mode detects a target strand without any amplification with complementary probe molecules immobilized on the cantilever surface using hybridization which induces stress in the microcantilever beam [18]. In comparison most current methods for oligonucleotide detection are limited owing to the length which is usually too small to anneal primers and generate amplicons or due to requirement of extensive time and material intensive routines. This has opened up the possibility of a novel platform for genomic studies using microcantilevers since oligonucleotide species can be detected directly using the static mode hybridization principle. The dynamic mode is based on measurement of change in the resonance frequency of the cantilever due to events on the cantilever surface or changes in the properties of the surrounding fluid. For the detection of oligonucleotides based on the dynamic mode, the maximum mass detectable under high degree of probe immobilization and hybridization efficiency conditions with target is still much lower than the current mass sensitivity [19]. Recently microcantilever based nanomechanical sensors have also demonstrated the ability to detect messenger RNA transcripts in a complex genomic background in the static mode [20]. This has paved way for the direct application of microcantilever sensors to functional genomic studies. The presence of competing species in hybridization based assays for single stranded nucleic acids is known to directly lower the sensitivity [21]. Hence for microcantilever-based assays to compete with established technologies, it is crucial to understand the sensor behavior in competitive backgrounds where non-specific interactions on the sensor layers are non-trivial.

Methods

Fragmentation of the universal human reference RNA (UHRR)

The total RNA (UHRR) (Agilent, USA) was provided in a solution of 70% ethanol and 0.1 M sodium acetate suspended in RNAase free water. Prior to fragmentation, the UHRR was extracted from this solution using the provided protocol from the manufacturer. The fragmentation of the UHRR was then carried out using the Bauer core protocol used for microarray and genechip assay [22] with a fragmentation time of 35 min. In order to maintain proper temperature, a thermal cycler was used (Techgene, Witeg, DE). After determining the concentration using UV-Vis (Nanodrop, USA) the final fragmented UHRR was suspended in DEPC water to a suitable concentration (generally higher than $1 \mu\text{g} \mu\text{l}^{-1}$) and immediately stored at -80°C for further use. After a PAGE gel analysis of the fragmentation efficiency and eventual distribution of strand length, the concentration of the fragmented RNA was calculated based on an average of 50 base pairs per molecule (16 104 daltons).

Probe preparation

For detecting complementary oligonucleotide sequence, thiolated probe molecules were designed with a thiol and $(\text{CH}_2)_6$ linker modifications at the 5' position of the phosphate group of a ssDNA and obtained from Microsynth (Balgach, CH). The thiolated probe molecules were suspended in a protective solution containing 0.01 mM dithiothreitol (DTT). Prior to using the probes for functionalization the DTT was extracted by using liquid–liquid extraction using diethyl ether (DEE) (Sigma Aldrich, DE) as the organic phase. The DTT molecules are relatively more soluble in the organic DEE phase and hence a multi-step extraction (5 \times) using fresh DEE at each step is used to remove DTT completely from the probe solution. Thereafter the aqueous phase was analyzed with the Nanodrop ND-1000 UV-Vis (Thermo Fischer, USA) to determine the probe concentration.

Functionalization solution and target sample preparation

All solutions were prepared in $18 \text{ M}\Omega \text{ cm}^{-1}$ Nanopure water (Thermo Fischer, DE) that was autoclaved twice (HMC, DE) and stored at 4°C . Probe thiolated ssDNA solutions at $20 \mu\text{M}$ were prepared in 50 mM triethyl ammonium acetate (TEAA) buffer (Sigma Aldrich, DE) for microcantilever functionalization. HSF71 match target and BioB2-C solutions at various concentrations were prepared for injection in the Gibco D-PBS, calcium/magnesium pH 7.2 $1 \times$ buffer (D-PBS) (Life Technologies, USA).

Microcantilever functionalization

Chipsets of microcantilever array sensors with eight sensors each were obtained from IBM Zurich research laboratory in Ruschlikon, Switzerland. The eight cantilevers are $500 \mu\text{m}$ in length, $100 \mu\text{m}$ in width and 500 nm in thickness fabricated at a pitch of $250 \mu\text{m}$. Sensor arrays were first exposed to 2 min atmospheric UV ozone cleaning (Boekel, USA). This was followed by a rinse in HPLC grade acetone (Sigma Aldrich, DE) for at least 30 min. After careful drying on a hot plate, the array was then cleaned in oxygen plasma cleaner (Diener PICO Barrel Asher, DE) for 3 min. The plasma operating parameters were 0.3 mbar O_2 at 160 W, 40 kHz power setting while using a custom made holder to ensure both sides of the cantilever sensors are cleaned. The sensors chips were subsequently coated on the top side with a 2 nm thick adhesive titanium layer and a 21 nm functional gold layer using 0.2 electron beam deposition tool (Temescal, USA). The titanium and gold were deposited at rates of 0.2 \AA s^{-1} and 0.5 \AA s^{-1} respectively to obtain an average grain size of $\sim 35 \text{ nm}$ and RMS roughness of 0.8 nm. The gold coated cantilevers were then individually functionalized by 30 min incubation in $20 \mu\text{M}$ of the respective thiolated probe solutions. This was followed by rinse in 50 mM TEAA and storage in the D-PBS $1 \times$ buffer at 4°C till further use usually within a day or maximum one week without loss of activity. This functionalization is the most crucial stage of the sensor preparation and needed a high level of optimization.

Measurement protocol

The functionalized cantilever was mounted into a flow cell containing the hybridization buffer Gibco D-PBS 1× before sealing the chamber. The laser deflection system is calibrated to correlate the absolute deflection of the cantilevers to the movement of the laser spot on the position sensitive detector [23]. The temperature of the measurement setup including the target samples and other solutions was kept at 21.5 °C in a thermally regulated enclosure and the sample was sucked through the chamber at a steady rate of 150 $\mu\text{l min}^{-1}$ using a programmed syringe pump (Genie Plus, Kent Scientific). Before the sample injection, the system was calibrated and normalized using a nanomechanical heat test peaking at ~ 2 °C for 10 s using a peltier heating element under the chamber. After a stable baseline was obtained under thermal equilibration, the sample was injected. The sensor was incubated in the solution as per the required assay followed by a buffer wash of at least 800 μl . As and when required, the sensor array was regenerated after this buffer wash with an injection of 800 μl of 4 M urea (Sigma Aldrich, DE) and incubation for at least 30 min. The sensor was then exposed to an excess wash of hybridization buffer before performing the next assay.

Results and discussion

We investigated the effects of target availability and background competition on the microcantilever differential sensor response so as to predict a quantitative model. To begin with, we first optimized the process for cantilever bio-functionalization. In comparison to the last known published results [24] we applied enhanced cantilever surface preparation using oxygen plasma, high precision and controlled deposition of the functional Au layer, surface activation of gold coated cantilevers using UV-ozone cleaning prior to functionalization with thiolated probe ssDNA and a new buffer for the *in situ* hybridization. In order to check the sensitivity of these sensors we determined the mechanical response to a range of ultra-low target concentrations from 10 pM down to 1 fM. Using micro-capillaries the microcantilever array was functionalized with thiolated probe ssDNA BioB2 (complementary to the target BioB2-C) while a random sequence of alternating adenosine-cytosine Unspec12 was used as a reference (table 1). A differential analysis of the signal obtained from the probe and the reference cantilevers is a prerequisite for an unbiased analysis of the sensor data since it accounts for absolute deflection signals arising from environmental changes in the sensor apparatus and the non-specific adsorption of molecules to non-active sensor interfaces [20]. The differential signal results only from the contribution of biomolecular interaction on the ssDNA functionalized gold interface. The surface biochemistry of the reference sensor should be identical to that of the probe cantilever but only lacking the specificity for target recognition. As shown in figures 1 and 2, the sensors detected the entire range selected for the analysis with all data points taken at 30 min from

Table 1. Thiolated probe ssDNA, their respective targets and references.

Oligos	Sequence	Function
Hsf71 match (probe)	SH—(CH ₂) ₆ —5'- ATG TGG AAA AAT ACC TAT TCT-3'	Match target gene Hsf71 match
Bio-B2 (probe)	SH—(CH ₂) ₆ —5'- TGC TGT TTG AAG-3'	Match sequence BioB2-C
Unspec24	SH—(CH ₂) ₆ —5'- ACA CAC ACA CAC ACA CAC ACA CAC-3'	Reference
Unspec12 (reference)	SH—(CH ₂) ₆ —5'- ACA CAC ACA CAC-3'	Unspecific sequence 12mer for reference cantilever
Hsf71 match (target)	5'-AGA ATA GGT ATT TTT CCA CAT-3'	Target sequence for Hsf71 match
BioB2-C (target)	5'-CTT CAA ACA GCA-3'	Complementary sequence for BioB2 probe

sample injection. As evident, the values do not represent saturation point since it was not within the scope of the study as a diagnostic technique to provide rapid results. The last reported limit for an identical analysis with the same set of probe and target and an identical set of cantilever arrays manufactured at IBM Zurich Laboratories (500 nm × 100 μm × 500 μm) was 10 pM with an average differential signal of ~ 10 nm [20]. Applying a new preparation and measurement protocol to the sensors we were clearly able to detect as low as 1 fM with an average differential signal of ~ 46 nm (four orders of magnitude improvement in sensitivity). Generally a Langmuir isotherm is fitted to the data in order to calculate the equilibrium constant from the steady state saturation values of concentration and deflection. Since this is not an equilibrium state analysis, we do not believe it is possible to derive detailed kinetic information from the data but the evaluation provides a semi-quantitative assessment of whether targets are present in the sample. We also performed an experiment with the same buffer (SSC 1×, 1 M NaCl) and other conditions used in the previous study for target concentration of 10 pM and found that the differential sensor response was still four fold higher which can be attributed to the functional gold layer activation. This is the first time a nanomechanical cantilever sensor has shown femtomolar sensitivity for an online *in situ* hybridization in pure target environments as compared to previous studies where the measurement was done offline [17].

After establishing the sensitivity of the nanomechanical sensors, we investigated the sensor response to non-specific competition in total fragmented UHRR with changing background and target concentrations. We chose here the Stratagene UHRR (Agilent Technologies, USA) which is extensively used as a reference in microarray technology [25]

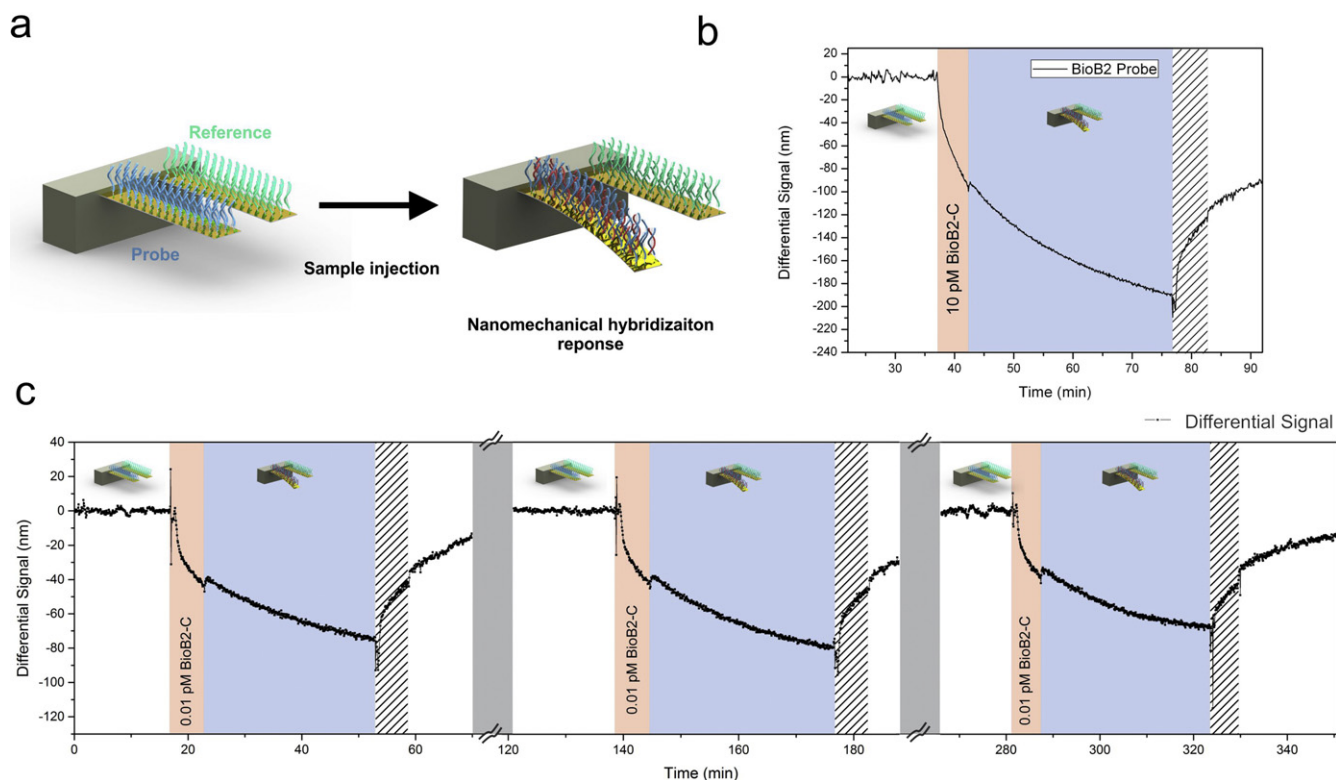


Figure 1. Detection of pure BioB2 target in a non-competitive sample buffer background against reference Unspec12. (a) Schematic of oligonucleotide detection using probe and reference microcantilevers. Hybridization of the target strand with the probe causes cantilever deflection and a differential response is determined by subtracting the reference from the probe cantilever deflection. (b) Differential signal for detection of 10 pM BioB2 target in Gibco PBS buffer. The pink areas indicate sample injection, blue area indicates incubation in sample and hashed area indicates buffer wash. (c) Differential signals for detection of target BioB2 at 0.01 pM concentration through three cycles with intermediate regeneration washes using 4 M urea incubation (gray area) showing reproducibility after sensor surface regeneration.

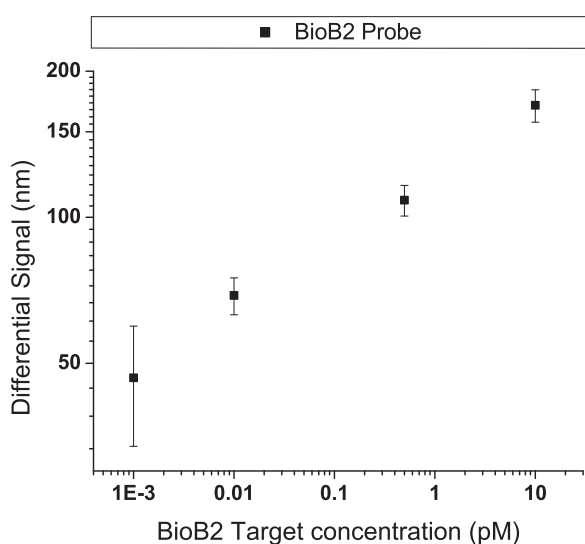


Figure 2. Differential BioB2 probe sensor response (log-scaled) to BioB2-C targets at concentrations ranging from 1 fM to 10 pM in Gibco PBS hybridization buffer against reference Unspec12. The data is gathered 30 min after injection of the sample for two different sets of cantilever arrays (both regenerated using 4 M urea) with at least three data points per assay.

and further fragment it using established protocols to keep the background comparable to other technologies used in genomic studies [20, 22]. This provides a strong competitive background to measure the response to an oligonucleotide target since it is a collection of fragmented RNAs. It is evident from the cell lines that compose the reference that the probability of finding a complete full length complementary strand for the HSF71 match probe is very minuscule given that the UHRRR was also fragmented. However there will be competition from partially complementary sequences that are known to significantly reduce response [26]. Although it has been shown that even SNP are clearly nanomechanically discriminable in total RNA [13, 20], the effect of background competition on SNP detection is not the aim of the present work. The sensor functionalization scheme includes thiolated 21 nucleotide probe HSF71 match, and an internal reference Unspec24 (table 1) immobilized on the cantilever surface. An internal positive control BioB2 was used in some experiments. The HSF71 probe sequence (21 base pairs matching the sense strand) is taken from a gene that encodes coagulation factor VII [27] in human blood which is a vitamin K-dependent factor essential for hemostasis, a mutation of which causes coagulopathy [28]. The respective targets are also listed in table 1. The probe and reference positional

arrangement on the cantilever arrays was randomized between different experiments. In order to ascertain the differential sensor response, the microcantilever arrays were exposed to HSf71 match (target) concentrations (10 pM, 100 pM and 500 pM) prepared for injection in the Invitrogen Gibco PBS 1× buffer with different fragmented UHRR concentrations (0 nM, 1 nM, 10 nM, 100 nM and 500 nM). The target concentrations were matched to the abundance of ncRNAs (miRNA etc) in biological samples [29, 30] so as to provide clinically relevant analysis. Recently the lower non-gold functionalized cantilever sides were altered to prevent non-specific adsorption which we consider an improvement [24]. The non-specific interactions of the molecules with the bare silicon cantilever surface can attribute to noise and a passivation of this side would be beneficial. However we did not include such protection in the current study since we were able to detect the targets in the required range without backside protection.

A detailed plot of the differential deflection versus the increasing background concentration for varying values of target concentration is shown in figure 3. All data points are taken at 30 min from sample injection time point and do not represent equilibrium values since the foremost aim is to provide a rapid and sensitive assay for oligonucleotides. Assuming the deflection signal (y) is proportional to the surface coverage of hybridized molecules [13], the data is fitted using the following logistic function similar to a dose response curve for competitive diagnostic immunoassays [31] as

$$y = \frac{A1 - A2}{1 + (x/x_0)^p} + A2 \quad (1)$$

Parameters: $A1$ —initial value, $A2$ —final value, x_0 —value of x when y is halfway between limiting values $A1$ and $A2$ and p —slope at inflection point x_0 . The initial limiting value $A1$ is evident at zero background concentration while the limiting final value $A2$ was fixed at 4.5 nm which is three times the inherent noise levels of detection (~ 1.5 nm). The model does not, in any way, represent a detailed kinetics based viewpoint of the system which is far more complex and currently not well understood for such systems [32, 33]. All parameters excluding $A2$ were allowed for the fitting. The final $A1$ values predicted with the model were in good agreement with the experimental data. Details of the fitting parameters are provided in table 2.

The value of x_0 is a strong indicator of the limits of the detection in background and sensor response to non-specific competition. For the 10 pM target concentration where x_0 is 1.37 nM, it indicates that the loss in signal at such low target concentrations is very rapid with increasing background when compared to higher concentrations ($x_0 = 49.88$ nM at 500 pM target level).

From the graph, it can hence be inferred that the deflection signal depends not only on the target concentration but also on the non-specific interaction from the background RNA. The competitive hybridization between different target and non-targets for the same probe can lead to steric

hindrance resulting in inhibition of target binding. The nature of the curve fitted to current data is asymptotic predicting a rather gradual loss of signal as the background concentration rises. There is however a limitation from experimental point of view since the detection limit set for 4.5 nm will not be reached till the background reaches tens of micromolar in concentration. Although this is not a steady state analysis and the mechanisms behind the cantilever deflection in competitive environments is barely known, it is still possible to quantify the range of operation of these sensors. There are practical considerations such as limitations of extracting total RNA from cell lines since amounts available for an assay are limited due to cell culture and extraction methods. Also, the amount of total RNA extracted depends on the method and the reagent of extraction. For example TRI® agent from Sigma Aldrich can yield 5–15 μg per million cells or 1–10 $\mu\text{g mg}^{-1}$ of tissue (a typical mammalian cell contains 10–30 pg total RNA). Additionally, an increase in noise levels in the optical deflection based detection can be observed with rise in background concentration [20]. Considering such limitations, it is possible that the sensors can be used for quantitative detection of oligonucleotides in as high as 5 μM background for a 10 pM 21 nt oligonucleotide target concentration (predicted sensor response of ~ 13 nm). The detection error (data spread) in both the cases (detection in competitive and no backgrounds) is a result of variability in the several steps leading up to experiment and might also be a result of variability in between different sensor chips. However despite this, it is apparent from the data and the resulting plots that it is still possible to clearly discriminate various concentrations of the target probe given that the background RNA concentration is well known.

Conclusions

We have for the first time demonstrated the femtomolar sensitivity of microcantilever based sensors for oligonucleotide detection in pure target environments. The enhancement is more than four orders of magnitude in liquids as compared to previous limits and paves way for ultrasensitive quantitative detection of oligonucleotides in an online method requiring no amplification or labeling of targets. We also profile here the effect of non-specific competition from total RNA on DNA probes while detecting ssDNA targets. The results are directly relevant to detection of any RNA/DNA oligonucleotide species since the interactions for detection of such targets are almost identical both being hybridization based approaches [34].

We have also provided a first insight into the effect of non-specific competition on the correlation between signal magnitude and target availability on label-free nanomechanical cantilever sensing based assays in a quantitative manner. Differences of response for exact complementary probes are observed in strong competition from random sequences. The simple dose response curve based modeling provides an insight into sensor response and can hence be used to assist the understanding of surface hybridization of DNA/RNA

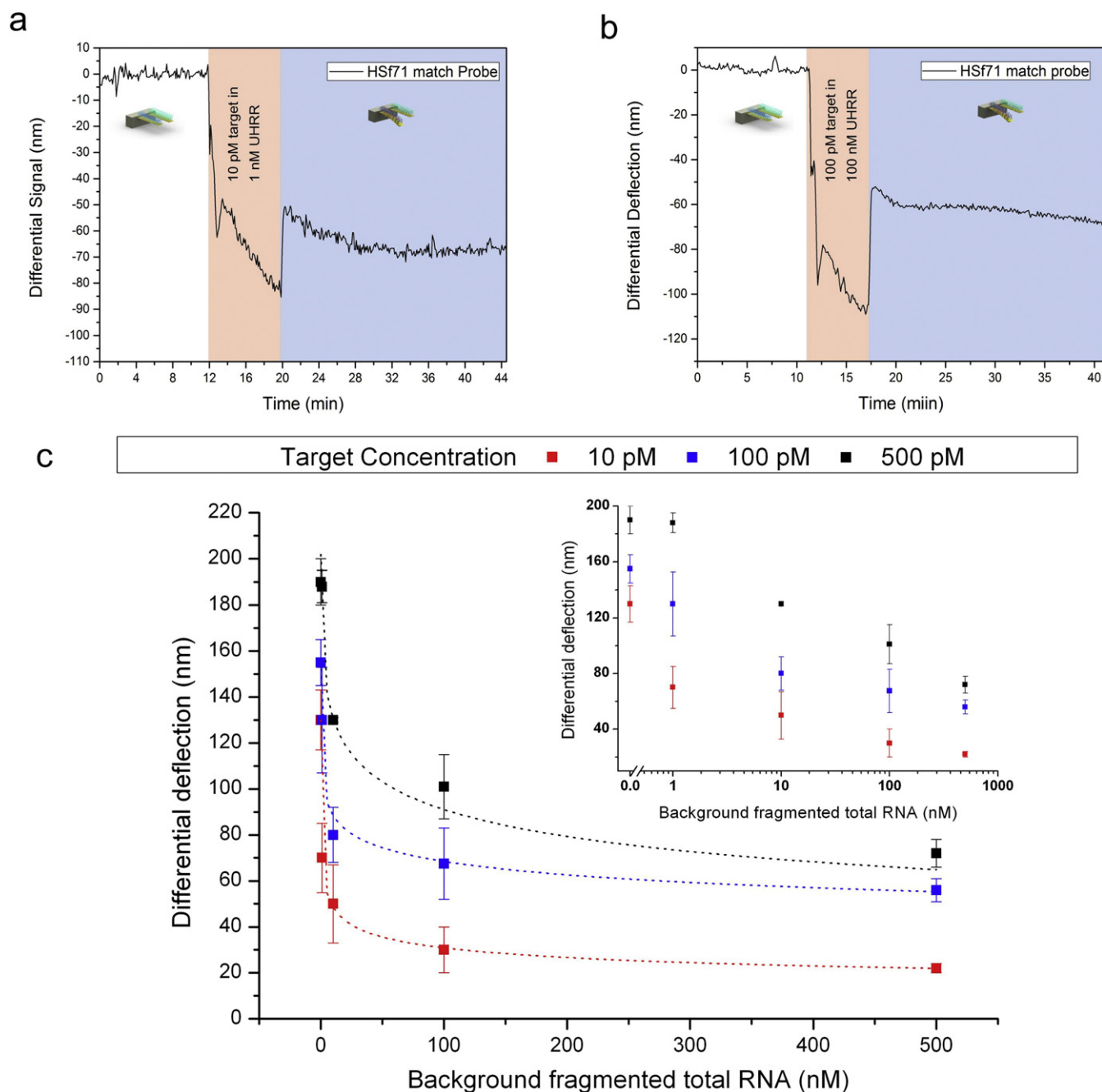


Figure 3. Effect of non-specific competition on nanomechanical assay of target oligonucleotide. (a) Detection of target HS71 match sequence in buffer at 10 pM concentration in 1 nM fragmented UHRR against reference Unspec24 (target has 21 nucleotides and reference has 24 nucleotides). The pink areas indicate sample injection while blue area indicates incubation in sample. (b) Detection of target HS71 match sequence in buffer at 100 pM concentration in 100 nM fragmented UHRR. (c) Detection of target HS71 match sequence at varying concentrations versus fragmented universal human reference RNA (total RNA) concentration (from no background to 500 nM fragmented UHRR concentration). Inset shows the same plot with a log x -axis for better representation. The graph indicates, as expected a drop in signal with a drop in the target concentration at any given value of background concentration. The analysis was based on average calculation of the differential signals after subtraction of individual cantilevers from an averaged reference. Three experiments were performed on two distinct sets of cantilever array chips. The rest of the data was gathered from distinct cantilever arrays with all having a minimum of three probe cantilever sensors per experiment.

molecules which remains a challenge especially in the presence of non-specific competition. The absolute concentrations evaluated in this study and their mechanical signal responses can be applied to compare the levels of expression and track life time variations in miRNA, siRNA and also

mRNA in direct competition or conjunction with current microarray technologies. Many microarray based formats may require noise reduction in addition to biological noise subtraction in order to provide a clearer representative plot for the sensor response [35, 36]. However, all data handling in

Table 2. Fitting parameters from equation (1) for background response of sensors. Values in the brackets indicate standard error.

Target concentration (pM)	Fitting parameters			
	A1 (nm)	A2 (nm)	p	x_0 (nM)
10	130 (1.12)	4.5	0.30 (0.00)	1.37 (0.17)
100	155.42 (8.64)	4.5	0.23 (0.06)	26.54 (23.76)
500	201.87 (27.85)	4.5	0.35 (0.11)	49.88 (47.52)

this study with static-mode microcantilever systems did not require such data smoothing (due to better signal to noise ratio), hence providing a possibility for reliable data on smaller variations in signal. This direct and label-free approach to sensing and quantification of single stranded nucleic acids can therefore provide a new platform in several areas from gene expression profiling, ncRNA pharmacokinetics (siRNA and miRNA), effect of chemical modification on gene silencing, detailed quantitative siRNA uptake assessment, miRNA quantification for disease monitoring and diagnosis etc.

The current study although performed on a eight cantilever per array sensor paves way for the possibility of having a highly multiplexed array with various probes and internal controls achieving high throughput comparable to current industry standards for quantitative hybridization based assays. With an understanding of sensor response in cellular RNA extracts being an important step towards such complex systems, we are currently working towards optimizing such systems for miniaturized multiplexed assays.

Acknowledgements

We are grateful to Science Foundation Ireland (SFI; SFI08/CE/I1432, SFI/09IN/1B2623) for their support.

References

- [1] Morozova O and Marra M A 2008 Applications of next-generation sequencing technologies in functional genomics *Genomics* **92** 255–64
- [2] Brenner S *et al* 2000 Gene expression analysis by massively parallel signature sequencing (MPSS) on microbead arrays *Nat. Biotechnol.* **18** 630–4
- [3] Pozhitkov A E, Bailey K D and Noble P A 2007 Development of a statistically robust quantification method for microorganisms in mixtures using oligonucleotide microarrays *J. Microbiol. Meth.* **70** 292–300
- [4] Bunimovich Y L, Shin Y S, Yeo W-S, Amori M, Kwong G and Heath J R 2006 Quantitative real-time measurements of DNA hybridization with alkylated nonoxidized silicon nanowires in electrolyte solution *J. Am. Chem. Soc.* **128** 16323–31
- [5] Phillips K S and Cheng Q 2007 Recent advances in surface plasmon resonance based techniques for bioanalysis *Anal. Bioanal. Chem.* **387** 1831–40
- [6] Anja B, Søren D, Stephan Sylvest K, Silvan S and Maria T 2011 Cantilever-like micromechanical sensors *Rep. Prog. Phys.* **74** 036101
- [7] Arlett J L, Myers E B and Roukes M L 2011 Comparative advantages of mechanical biosensors *Nat. Nanotechnology* **6** 203–15
- [8] Fritz J, Baller M K, Lang H P, Rothuizen H, Vettiger P, Meyer E, Güntherodt H-J, Gerber C and Gimzewski J K 2000 Translating biomolecular recognition into nanomechanics *Science* **288** 316–8
- [9] Rijal K and Mutharasan R 2007 PEMC-based method of measuring DNA hybridization at femtomolar concentration directly in human serum and in the presence of copious noncomplementary strands *Anal. Chem.* **79** 7392–400
- [10] Tamayo J, Kosaka P M, Ruz J J, San Paulo A and Calleja M 2013 Biosensors based on nanomechanical systems *Chem. Soc. Rev.* **42** 1287–311
- [11] Li X X and Lee D W 2012 Integrated microcantilevers for high-resolution sensing and probing *Meas. Sci. Technol.* **23** 022001
- [12] Backmann N, Zahnd C, Huber F, Bietsch A, Plückthun A, Lang H-P, Güntherodt H-J, Hegner M and Gerber C 2005 A label-free immunosensor array using single-chain antibody fragments *Proc. Natl. Acad. Sci. USA* **102** 14587–92
- [13] McKendry R *et al* 2002 Multiple label-free biodetection and quantitative DNA-binding assays on a nanomechanical cantilever array *Proc. Natl. Acad. Sci.* **99** 9783–8
- [14] Braun T, Ghatkesar M K, Backmann N, Grange W, Boulanger P, Letellier L, Lang H-P, Bietsch A, Gerber C and Hegner M 2009 Quantitative time-resolved measurement of membrane protein–ligand interactions using microcantilever array sensors *Nat. Nanotechnology* **4** 179–85
- [15] Mader A, Gruber K, Castelli R, Hermann B A, Seeberger P H, Rädler J O and Leisner M 2011 Discrimination of *Escherichia coli* strains using glycan cantilever array sensors *Nano Lett.* **12** 420–3
- [16] Nugaeva N, Gfeller K Y, Backmann N, Düggelein M, Lang H P, Güntherodt H-J and Hegner M 2007 An antibody-sensitized microfabricated cantilever for the growth detection of *Aspergillus niger* spores *Microsc. Microanal.* **13** 13–7
- [17] Mertens J, Rogero C, Calleja M, Ramos D, Martin-Gago J A, Briones C and Tamayo J 2008 Label-free detection of DNA hybridization based on hydration-induced tension in nucleic acid films *Nat. Nanotechnology* **3** 301–7
- [18] Lang H P, Hegner M, Meyer E and Ch G 2002 Nanomechanics from atomic resolution to molecular recognition based on atomic force microscopy technology *Nanotechnology* **13** R29
- [19] Jensen J, Maloney N and Hegner M 2013 A multi-mode platform for cantilever arrays operated in liquid *Sensor. Actuat. B-Chem.* **183** 388–94
- [20] Zhang J, Lang H P, Huber F, Bietsch A, Grange W, Certa U, McKendry R, Güntherodt H J, Hegner M and Gerber Ch 2006 Rapid and label-free nanomechanical detection of biomarker transcripts in human RNA *Nat. Nanotechnology* **1** 214–20
- [21] Halperin A, Buhot A and Zhulina E B 2004 Sensitivity, specificity, and the hybridization isotherms of DNA chips *Biophys. J.* **86** 718–30

- [22] Schinke-Braun M and Couget J 2007 *Cardiac Gene Expression* ed J Zhang and G Rokosh (New York: Springer) pp 13–40
- [23] Mishra R, Grange W and Hegner M 2012 Rapid and reliable calibration of laser beam deflection system for microcantilever-based sensor setups *J. Sensors* **2012** 6
- [24] Huber F, Lang H P, Backmann N and Rimoldi D Gerber Ch 2013 Direct detection of a BRAF mutation in total RNA from melanoma cells using cantilever arrays *Nat. Nanotechnology* **8** 125–9
- [25] Canales R D *et al* 2006 Evaluation of DNA microarray results with quantitative gene expression platforms *Nat. Biotechnol.* **24** 1115–22
- [26] Hansen K M, Ji H F, Wu G, Datar R, Cote R, Majumdar A and Thundat T 2001 Cantilever-based optical deflection assay for discrimination of DNA single-nucleotide mismatches *Anal. Chem.* **73** 1567–71
- [27] Tan C W, Najm J, Morel-Kopp M C, Teo J, Chen Q, Felbor U and Ward C M 2012 Severe FX deficiency caused by a previously unidentified 4-bp deletion compound heterozygous with a large deletion involving FVII and FX genes *Haemophilia* **18** e55–8
- [28] Raobaikady R, Redman J, Ball J A S, Maloney G and Grounds R M 2005 Use of activated recombinant coagulation factor VII in patients undergoing reconstruction surgery for traumatic fracture of pelvis or pelvis and acetabulum: a double-blind, randomized, placebo-controlled trial *Brit. J. Anaesth.* **94** 586–91
- [29] Mitchell P S *et al* 2008 Circulating microRNAs as stable blood-based markers for cancer detection *Proc. Natl. Acad. Sci.* **105** 10513–1058
- [30] Wang J, Yi X, Tang H, Han H, Wu M and Zhou F 2012 Direct quantification of microRNA at low picomolar level in sera of glioma patients using a competitive hybridization followed by amplified voltammetric detection *Anal. Chem.* **84** 6400–6
- [31] Wild D 2013 *The Immunoassay Handbook: Theory and Applications of Ligand Binding, ELISA and Related Techniques* (Oxford: Elsevier)
- [32] Held G A, Grinstein G and Tu Y 2003 Modeling of DNA microarray data by using physical properties of hybridization *Proc. Natl Acad. Sci.* **100** 7575–780
- [33] Burden C J and Binder H 2010 Physico-chemical modelling of target depletion during hybridization on oligonucleotide microarrays *Phys. Biol.* **7** 016004
- [34] Nakano S-i, Fujimoto M, Hara H and Sugimoto N 1999 Nucleic acid duplex stability: influence of base composition on cation effects *Nucleic Acids Res.* **27** 2957–65
- [35] Halper-Stromberg E *et al* 2011 Performance assessment of copy number microarray platforms using a spike-in experiment *Bioinformatics* **27** 1052–60
- [36] Luscombe N M, Royce T E, Bertone P, Echols N, Horak C E, Chang J T, Snyder M and Gerstein M 2003 Express yourself: a modular platform for processing and visualizing microarray data *Nucleic Acids Res.* **31** 3477–82